EPJ Web of Conferences **364**, 08009 (2026) https://doi.org/10.1051/epjconf/202636408009
Quark Matter 2025

Prompt/Non-prompt J/ψ production in pp collisions at forward and midrapidity with ALICE

Shreyasi Acharya[1,*] for the ALICE Collaboration
[1]Sezione INFN, Bari, Italy

Abstract. Quarkonium production in high-energy hadronic collisions is sensitive to both perturbative and non-perturbative aspects of quantum chromodynamics (QCD) calculations. The charmonium cross section can be split into prompt and non-prompt components, the first corresponding to directly produced charm-anticharm pairs, the second originating from the decay of beauty hadrons. Both components are relevant for the investigation of the properties of the quark–gluon plasma (QGP), with the latter allowing to study the mass dependence of heavy quarks in-medium energy-loss mechanism. In this contribution the recent measurement of prompt and non-prompt J/ψ carried out by the ALICE Collaboration in pp ($|y| < 0.8$) will be shown, including the newest results from LHC Run 3. Moreover, thanks to the installation of the new muon forward tracker (MFT), prompt/non-prompt charmonium separation is now possible in LHC Run 3 at forward rapidity ($2.5 < y < 3.6$). In pp collisions at $\sqrt{s} = 13.6$ TeV, the first results on the non-prompt J/ψ fraction with respect to prompt J/ψ at forward rapidity in ALICE are presented.

1 Introduction

In ultrarelativistic ion collisions at LHC energies, heavy quarks (charm and beauty) are produced very early in the collisions (formation times: $\tau_c \sim 0.08$ fm/c, $\tau_b \sim 0.02$ fm/c) via hard scattering processes. Bound states of a heavy quark and antiquark, called quarkonia, appear as different particles depending on their quantum state, binding energy, and spatial radius; J/ψ being the lowest vector meson state formed from a charm–anticharm pair. Heavy quark production is treated perturbatively, since their bare masses ($m_{\mathrm{c}} \sim 1.3$ GeV/c^2, $m_{\mathrm{b}} \sim 4.2$ GeV/c^2) are much larger than the QCD scale parameter ($\Lambda_{\mathrm{QCD}} \simeq 200$ MeV). Quarkonium bound states, however, are treated non-relativistically due to the low velocity of the quarks, making non-relativistic potential models suitable. Several theoretical approaches have been proposed to describe quarkonium production in vacuum. In the Color Singlet Model (CSM) [1], quarkonia form directly in a colour-singlet state; in Non-relativistic QCD (NRQCD) [2], formation proceeds via both colour-singlet and colour-octet states; and in the Color Evaporation Model (CEM) [3], a quarkonium forms if the invariant mass of the quark pair ($m_{Q\bar{Q}}$) is below the open heavy-flavour threshold, independent of the colour state.

*e-mail: shreyasi.acharya@cern.ch

2 ALICE upgrade for Run 3

The ALICE detector system has undergone several upgrades to enable high-intensity data taking for the LHC operations starting from 2022 (Run 3) [4]. The major upgrades relevant to these results involve the Inner Tracking System (ITS), the Time Projection Chamber (TPC) in the midrapidity region ($|\eta| < 0.9$), and the installation of a new tracking detector, the Muon Forward Tracker (MFT), in the forward rapidity region ($-3.6 < \eta < -2.5$). The upgraded ITS [5] employs Monolithic Active Pixel Sensor (MAPS) technology with seven layers, increasing the readout rate to ~100 kHz for Pb–Pb collisions, compared to ~1 kHz previously. The MultiWire Proportional Chamber (MWPC) readout units of the TPC [6] have been replaced with Gas Electron Multiplier (GEM) detectors, raising its readout rate capabilities to 50 kHz from only a few kHz. The MFT [7] detector has been installed before the front absorber, at 0.46 m from the nominal interaction point, which allows muon tracks to be associated with the primary vertex and improves the vertex resolution of forward tracks. This enables, for the first time in ALICE, the separation of prompt and non-prompt J/ψ at forward rapidity.

3 Analysis technique

J/ψ mesons are classified in two groups according the distance of their production from the primary vertex. Prompt J/ψ are produced immediately after the collision, with decay lengths of a few picometers, either directly from a $c\bar{c}$ pair or indirectly via decays of higher charmonium states like χ_c or $\psi(2S)$. Non-prompt J/ψ come from beauty-hadron decays, with decay lengths in the order of a few hundred micrometres e.g. $c\tau_{B^+} \sim 500\ \mu$m. The

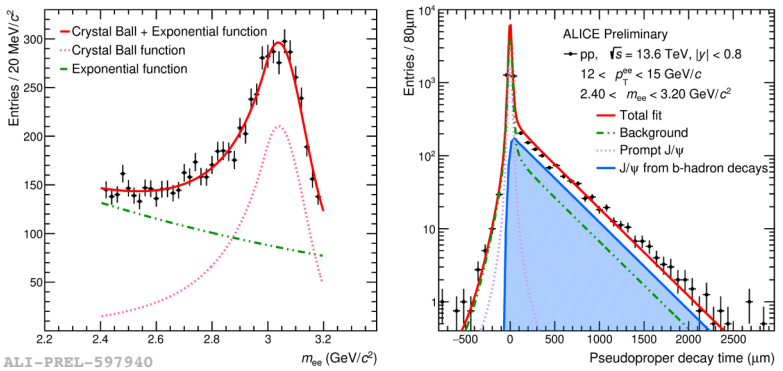

Figure 1. Simultaneous likelihood fit to the invariant mass (left) and pseudoproper decay length (right) distributions of dielectrons in $12 < p_{\mathrm{T}}^{ee} < 15$ GeV/c for pp collisions at $\sqrt{s} = 13.6$ TeV.

non-prompt fraction, f_B, is extracted via a simultaneous maximum-likelihood fit to the two-dimensional distribution of invariant mass and pseudoproper decay length, as illustrated in Fig. 1 for dielectrons within $12 < p_{\mathrm{T}}^{ee} < 15$ GeV/c in pp collisions at $\sqrt{s} = 13.6$ TeV. The invariant mass (m_{ee}) is fitted with a Crystal Ball function for the signal and an exponential for the background, while the pseudoproper decay length (x) is modeled with a background function taken from [8], along with signal templates for prompt and non-prompt contributions from simulations. The prompt and non-prompt J/ψ cross sections are estimated as:

$$\frac{\mathrm{d}^2N}{\mathrm{d}y\mathrm{d}p_{\mathrm{T}}}^{\text{Prompt } J/\psi} = (1 - f_B) \times \frac{\mathrm{d}^2N}{\mathrm{d}y\mathrm{d}p_{\mathrm{T}}}^{\text{Inclusive } J/\psi}, \qquad \frac{\mathrm{d}^2N}{\mathrm{d}y\mathrm{d}p_{\mathrm{T}}}^{J/\psi \leftarrow h_B} = f_B \times \frac{\mathrm{d}^2N}{\mathrm{d}y\mathrm{d}p_{\mathrm{T}}}^{\text{Inclusive } J/\psi}$$

4 Results and Discussions

Figure 2 shows the p_{T}-differential cross sections of prompt and non-prompt J/ψ at midrapidity ($|y| < 0.9$) in pp collisions at $\sqrt{s} = 13$ TeV from the Run 2 data [9]. Predictions from NRQCD-based models [10] and improved CEM with the k_{T}-factorisation approach [11] describe the prompt J/ψ data well, while the FONLL (Fixed-Order Next-to-Leading Log) [12] perturbative calculation provides a good description of the non-prompt J/ψ data within uncertainties. Figure 3 shows the fraction of non-prompt J/ψ relative to prompt J/ψ as a function

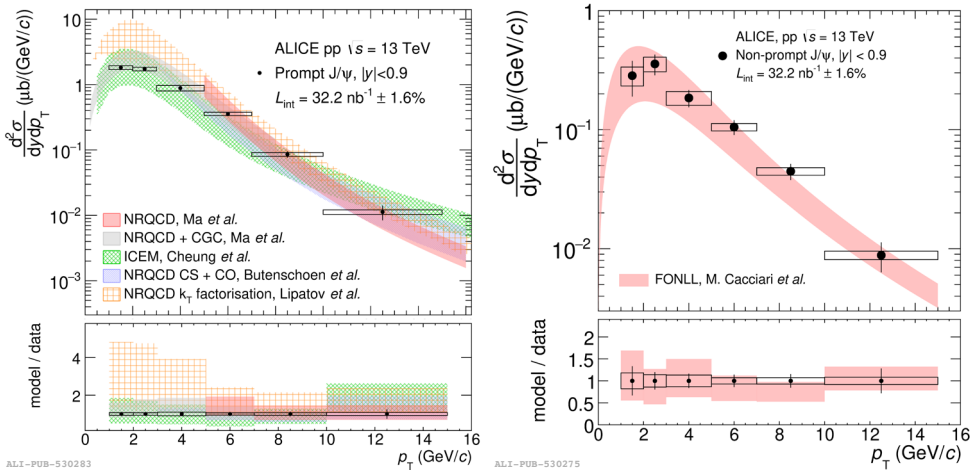

Figure 2. p_T-differential cross sections of prompt (left) and non-prompt (right) J/ψ within $|y| < 0.9$ in pp collisions at $\sqrt{s} = 13$ TeV.

of transverse momentum in pp collisions at $\sqrt{s} = 13.6$ TeV. The left panel shows f_{B} at midrapidity ($|y| < 0.9$) from dielectron reconstruction, with Run 3 results in good agreement with Run 2 at $\sqrt{s} = 13$ TeV. The upgraded detector and higher luminosity in Run 3 allow much finer granularity in p_{T}. The right panel presents the first ALICE measurement of the non-

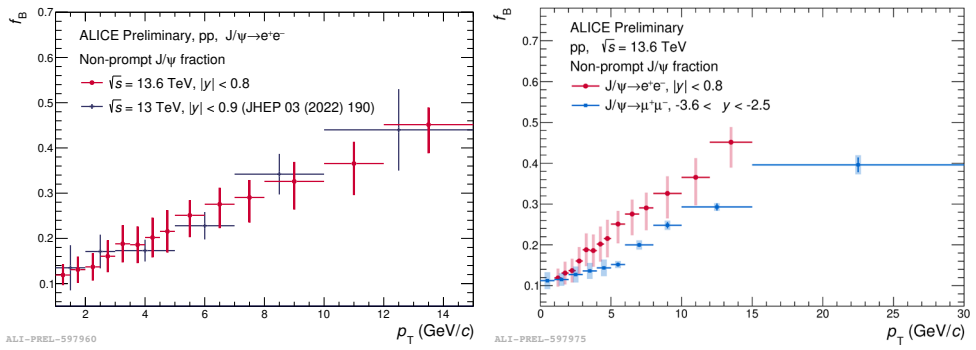

Figure 3. Non-prompt J/ψ fraction as a function of transverse momentum in pp collisions at $\sqrt{s} = 13.6$ TeV at mid ($|y| < 0.9$) and forward ($-3.6 < \eta < -2.5$) rapidities.

prompt J/ψ fraction at forward rapidity ($-3.6 < \eta < -2.5$), possible due to the new MFT

detector. The non-prompt fraction increases with p_{T} for both rapidity regions, with a more pronounced rise at midrapidity, consistent with the stronger production of $b\bar{b}$ at midrapidity compared to forward rapidity. The left panel of Fig. 4 shows that the ALICE results are consistent with the ATLAS [13] and LHCb [14] measurements at both mid and forward rapidities. ALICE extends the coverage down to $p_{\mathrm{T}} = 1$ GeV/c, complementing ATLAS measurements at high p_{T}. The right panel of Fig. 4 shows that PYTHIA with default color reconnection [15] describes the midrapidity data within uncertainties. No significant differences are observed among PYTHIA versions, including v8.311 [16] implementing quarkonium production via NRQCD in a timelike parton shower, up to $p_{\mathrm{T}} \sim 11$ GeV/c. Although at higher p_{T}, both versions of PYTHIA predictions appear to deviate from data, no firm conclusion can be drawn due to limited Monte Carlo statistics at such p_{T}.

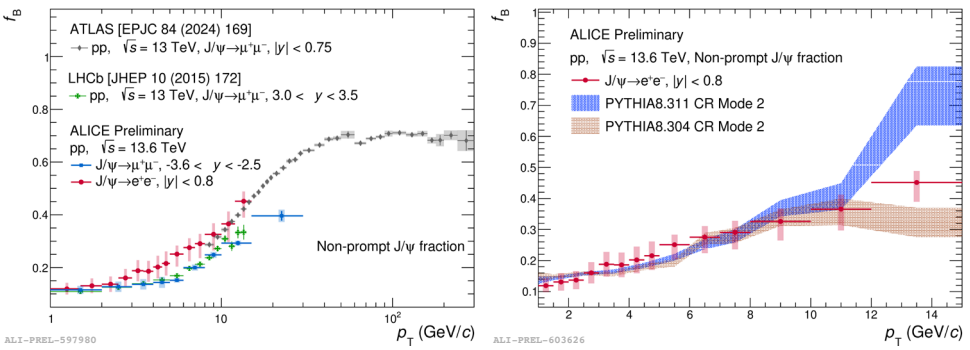

Figure 4. Non-prompt J/ψ fraction from ALICE compared with measurements from ATLAS and LHCb (left) and PYTHIA Monte Carlo predictions (right).

References

[1] H Fritzsch., PLB 67 (1977) 217
[2] G. T. Bodwin et. al., PRD 51 (1995) 1125; Erratum: PRD 55 (1997), 5853
[3] R. Baier & R. Ruckl, PLB 102 (1981) 364; F. Amundson et. al., PLB 390 (1997) 323
[4] ALICE Collaboration, JINST 19 (2024) P05062
[5] ALICE Collaboration, CERN-LHCC-2013-024; ALICE-TDR-017
[6] ALICE Collaboration, CERN-LHCC-2013-020; ALICE-TDR-016
[7] ALICE Collaboration, CERN-LHCC-2015-001; ALICE-TDR-018
[8] CDF Collaboration, PRD 71 (2005) 032001
[9] ALICE Collaboration, JHEP 03 (2022) 190
[10] M. Butenschoen & B. A. Kniehl, PRL 106 (2011) 022003; Y. Q. Ma et. al, PRL 106 (2011) 042002; S. Baranov & A. Lipatov, PRD 100 (2019) 114021; Y. Q. Ma & R. Venugopalan, PRL 113 (2014) 192301
[11] V. Cheung & R. Vogt, PRD 98 (2018) 114029
[12] M. Cacciari et. al., JHEP 05 (1998) 007; M. Cacciari et. al., JHEP 10 (2012) 137
[13] ATLAS Collaboration, EPJC 84 (2024) 169
[14] LHCb Collaboration, JHEP 10 (2015) 172, 2015
[15] T. Sjostrand et. al., Comput. Phys. Commun. 191, 159 (2015)
[16] N. Cooke et.al., EPJC (2024) 84, 432